ARRAY ELEMENT LOCALIZATION ACCURACY AND SURVEY DESIGN

Stan E. Dosso[1] and Gordon R. Ebbeson[2]
[1]School of Earth and Ocean Sciences, University of Victoria, Victoria BC, Canada, V8W 3P6, sdosso@uvic.ca
[2]Defence Research and Development Canada–Atlantic, Dartmouth NS, Canada, B2Y 3Z7

1. INTRODUCTION

Advanced array processing methods in underwater acoustics require knowledge of the locations of individual elements in a sensor array. However, sufficiently accurate sensor locations are often not known after array deployment, and array element localization (AEL) surveys are required. AEL is based on inverting acoustic arrival-time measurements from a series of controlled sources to the sensors to be localized [1, 2]. AEL is usually based on direct acoustic paths, but can also include surface and/or seabed reflected paths to provide more information. Synchronized AEL surveys, in which the source transmission times are known, are more complicated logistically than non-synchronized surveys, but provide more informative data. AEL accuracy also depends on a number of other factors including arrival time uncertainty, number of sources, source configuration, source-position uncertainties, and water-column sound-speed and depth uncertainties.

This paper quantifies sensor-localization accuracy in terms of an analytic result for the posterior uncertainties of a Bayeisan formulation of AEL inversion which takes all of the above factors into account. This provides a rigorous and general measure of the accuracy that can be achieved in AEL applications without resorting to computationally-intensive Monte Carlo simulations. The approach can be applied to study the relative importance of the various factors influencing AEL accuracy, and to guide in planning efficient and effective AEL surveys.

2. THEORY

2.1 Inverse Theory

Let $\mathbf{d}$ and $\mathbf{m}$ be vectors of measured data and unknown model parameters, respectively, with the elements of each considered to be random variables. According to Bayes' rule, the posterior probability density (PPD) $P(\mathbf{m}|\mathbf{d})$ is then proportional to the product of the likelihood function (quantifying data information) and the prior probability distribution (expressing independent model information). Assuming that the errors (uncertainties) for the measured data and prior parameter estimates $\hat{\mathbf{m}}$ are Gaussian-distributed random variables with covariance matrices $\mathbf{C_d}$ and $\mathbf{C}_{\hat{\mathbf{m}}}$ (typically diagonal matrices with variances on the main diagonal), the PPD may be expressed

$$P(\mathbf{m}\,|\,\mathbf{d}) \propto \exp\{-[(\mathbf{d}-\mathbf{d}(\mathbf{m}))^T \mathbf{C}_\mathbf{d}^{-1}(\mathbf{d}-\mathbf{d}(\mathbf{m})) + (\hat{\mathbf{m}}-\mathbf{m})^T \mathbf{C}_{\hat{\mathbf{m}}}^{-1}(\hat{\mathbf{m}}-\mathbf{m})]/2\}, \quad (1)$$

where $\mathbf{d}(\mathbf{m})$ represents data predicted for model $\mathbf{m}$. For a linear problem with $\mathbf{d}(\mathbf{m}) = \mathbf{Am}$, the maximum *a posteriori* (MAP) solution (i.e., the most probable parameter set) is found by setting the PPD derivative to zero, leading to

$$\mathbf{m} = [\mathbf{A}^T\mathbf{C}_\mathbf{d}^{-1}\mathbf{A} + \mathbf{C}_{\hat{\mathbf{m}}}^{-1}]^{-1}\mathbf{A}^T\mathbf{C}_\mathbf{d}^{-1}[\mathbf{d}-\mathbf{A}\hat{\mathbf{m}}]. \quad (2)$$

Further, the PPD is a multi-dimensional Gaussian distribution with expected values given by the MAP parameters and posterior covariance matrix

$$\mathbf{C_m} = [\mathbf{A}^T\mathbf{C}_\mathbf{d}^{-1}\mathbf{A} + \mathbf{C}_{\hat{\mathbf{m}}}^{-1}]^{-1}. \quad (3)$$

In particular, the standard deviation for parameter m_i is given by the square-root of the ith diagonal element of $\mathbf{C_m}$.

2.2 AEL Inversion

A general formulation of AEL inversion includes as unknown parameters not only the positions (x, y, z) of the sensors to be localized, but also source locations and water-column parameters to properly account for the effect of uncertainties in these quantities. Source transmission instants can be treated as either unknown, known, or known to within a common timing offset to account for system synchronization error. Treating the above quantities as unknown parameters leads to an under-determined inverse problem. However, incorporating prior estimates with uncertainties, as outlined above, regularizes the inversion and provides a stable, well-determined solution and quantitative posterior uncertainty estimates. AEL is based on inverting the acoustic ray-tracing equations

$$t = \int_{\text{ray path}} \frac{dz}{c(z)[1-p^2c^2(z)]^{1/2}}, \quad (4)$$

$$r = \int_{\text{ray path}} \frac{pc(z)dz}{[1-p^2c^2(z)]^{1/2}}. \quad (5)$$

In Eq. (5), the arrival time data t are equal to the transmission time t_0 plus the travel time along the ray path through sound-speed profile $c(z)$ (possibly including surface

and/or bottom reflections). Ray parameters $p = \cos\theta(z)/c(z)$ (θ is grazing angle) for eigenrays connecting source and receiver are determined by searching for values which produce the correct range r via Eq. (6). An efficient search uses Newton's method to refine an initial approximation based on straight-line propagation, with boundary reflections incorporated using the method of images [1].

The ray equations are functionally nonlinear, but can be linearized using a truncated Taylor-series expansion about an arbitrary starting model $\mathbf{m_0}$, leading to a MAP estimate

$$\mathbf{m} = [\mathbf{J}^T\mathbf{C}_\mathbf{d}^{-1}\mathbf{J} + \mathbf{C}_{\hat{\mathbf{m}}}^{-1}]^{-1}\mathbf{J}^T\mathbf{C}_\mathbf{d}^{-1}[\mathbf{t} - \mathbf{t}(\mathbf{m}_0) + \mathbf{J}(\mathbf{m}_0 - \hat{\mathbf{m}})], \quad (6)$$

where $\mathbf{J}$ is the Jacobian matrix of partial derivatives with elements $J_{ik} = \partial t_i(\mathbf{m_0})/\partial m_k$. Due to the linearization, the inversion must be repeated iteratively to convergence [1, 2]. Parameter uncertainties are given by Eq. (4) with $\mathbf{J}$ (evaluated at the final model) substituted for $\mathbf{A}$ and $\mathbf{t}$ for $\mathbf{d}$. The required integrals and derivatives can be derived analytically for a piecewise-linear sound-speed profile [1].

3. AEL EXAMPLE

As a synthetic AEL example, Fig. 1(a) shows a plan view of a 30-element horizontal sensor array (at 75-m depth) together with 8 acoustic sources (30-m depth). Fig. 1(b) shows the sound-speed profile, and Fig. 1(c) shows ray paths with up to one bottom reflection for the maximum range of 800 m. In this example, arrival time uncertainties are 0.5 ms and prior information consists of source locations known to within 10 m in x and y and 5 m in z, and sensor locations known to within 50 m in x and y and 10 m in z.

Fig. 2 shows that posterior sensor-location uncertainties for direct-path AEL inversion are smaller by up to ~1.5 m for known source-transmission timing over unknown timing. Results for timing known to within a constant offset are similar to known timing. The unknown timing results degrade (relative to known timing) for cases involving fewer sources or inferior source geometries (not shown).

Fnally, Fig. 3 shows mean sensor-location uncertainties computed using different acoustic arrivals (d—direct, s—surface-reflected, b—bottom-reflected, all—all paths in Fig. 1c) and various water-depth uncertainties. Sensor depth is improved most by including reflected arrivals (since these have different vertical angles but follow the same x-y paths as direct arrivals); however, the benefits of bottom-reflected paths diminish with increasing water-depth uncertainty.

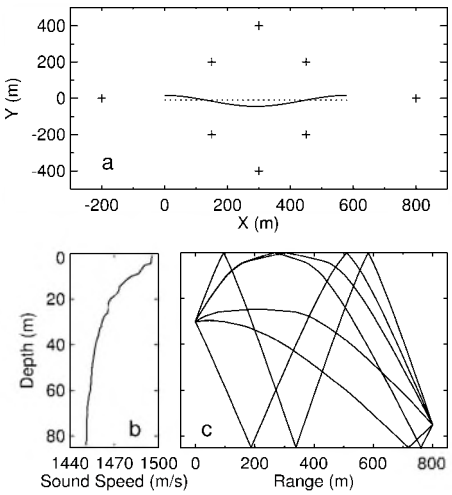

Fig. 1. AEL example: (a) plan view of array (solid line) compared to straight (dotted) line and source positions (crosses); (b) sound-speed profile; and (c) ray paths with up to one bottom reflection.

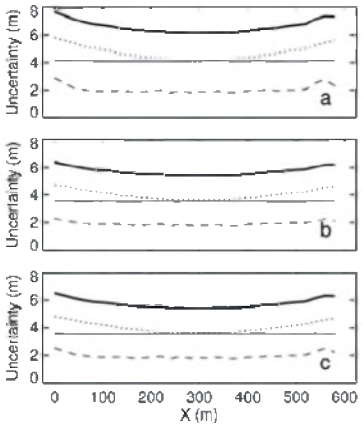

Fig. 2. Posterior sensor-location uncertainties in x, y, z and $R=[x^2+y^2+z^2]^{1/2}$ (solid, dotted, dashed and heavy solid lines, respectively) when transmission times are (a) unknown, (b) known, and (c) known to within a common offset.

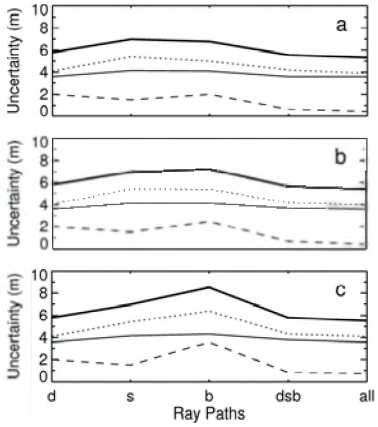

Fig. 3. Mean sensor-location uncertainties in x, y, z and R (solid, dotted, dashed and heavy solid lines, respectively) for indicated ray paths when the water-depth uncertainty is 1, 2 and 5 m in (a), (b) and (c), respectively.

REFERENCES

[1] S.E. Dosso & N.E. Collison (2001). Regularized inversion for towed-array shape estimation. *Inverse Problems in Underwater Acoustics*, Eds: M.I. Taroudakis & G.N. Makrakis (Springer-Verlag, New York), 77–103.

[2] S.E. Dosso, N.E. Collison, G.J. Heard & R.I. Verrall (2004). Experimental validation of regularized array element localization. *J. Acoust. Soc. Am*, **115**, 2129–2137.